



Observation of nocturnal NO₃ during vehicular activities in the medium sized city of Calicut in coastal India

Kuttoth Suhail¹, Ramachandran Arun^{1*}, Shreya Joshi³, John Shebin¹, Saseendran Aiswarya¹, Pakkattil Anoop¹, Viswanath Deepa², Ravi Varma¹

5 ¹Department of Physics, National Institute of Technology Calicut, Calicut, 673601, India

²Department of Physics, VTM NSS College, Trivandrum, 695503, India

³Optind Solutions Pvt. LTD., Unit 11, Technology Business Incubator, National Institute of Technology Calicut, Calicut, 673601, India

10 *Correspondence to: R. Arun (arunrpkd@gmail.com)

Abstract. Nitrate radical (NO₃) is the most important nocturnal oxidant in urban atmosphere. The city of Calicut (Kozhikode) is a medium sized urban location in India. One of the bus terminals at Palayam part of the city [11.2495° N, 75.7842° E] is adjacent to the vegetable sorting facilities cum market, both of which have intense activities by buses and trucks from about 3 AM till about 8 PM on all working days. We report preliminary measurements observing NO₃ on five nights during a weeklong measurement campaign in the autumn of 2018. Measurements were made between 10 PM and 6 AM, and focus was when diesel vehicles were found idling along about half a km stretch during 3 – 6 AM while the loading/unloading of vegetables at sorting facility happens. Incoherent Broadband Cavity Enhanced Absorption Spectroscopic technique in open-path configuration (OP-IBBCEAS) was employed for measurements. The instrument was installed 8.5 m above the ground level over the east wing of Palayam bus terminal building adjacent to the vegetable market. The 285 cm long optical resonator was arranged on a custom-made aluminium profile platform 1 m high. The stability of the instrument for the entire period of measurement was excellent, and high NO₃ mixing ratios with levels exceeding several hundred pptv were observed during early morning hours when heavy vehicles were idling. The highest NO₃ mixing ratio observed was (497 ± 140) pptv during one of the nights. The fit uncertainty, which was considered as the uncertainty in retrieved concentration, was found to increase with increased aerosol loading. The uncertainty for a spectral averaging interval of 10 min was recorded as ~20 pptv and ~100 pptv during the lowest and the highest aerosol loading events respectively.

1 Introduction

The photochemistry of the atmosphere induced by sunlight triggers the formation of various free radicals, like nitrate and hydroxyl radicals and other vital trace gas species [Bohn et al., 2005; Monks et al., 2005]. The day and night time chemistry of the atmosphere are different and the in situ monitoring of the radical species are essential because of their high reactivity and short lifetimes [Khan et al., 2015; Larin et al., 2014; Geyer et al., 2003]. The adverse health impacts of these trace gases



have also been recognized as far reaching [Sarnat, 2016]. Being a dominant night-time oxidant, NO_3 triggers the formation of other trace species like nitric acid and peroxy radicals [Wayne et al., 1991; Atkinson, 1991]. It reacts with various hydrocarbons and enhances VOC oxidations [Khan et al., 2015]. The presence of NO_3 is an indication of VOCs (source) and N_2O_5 (sink) in the atmosphere.

5

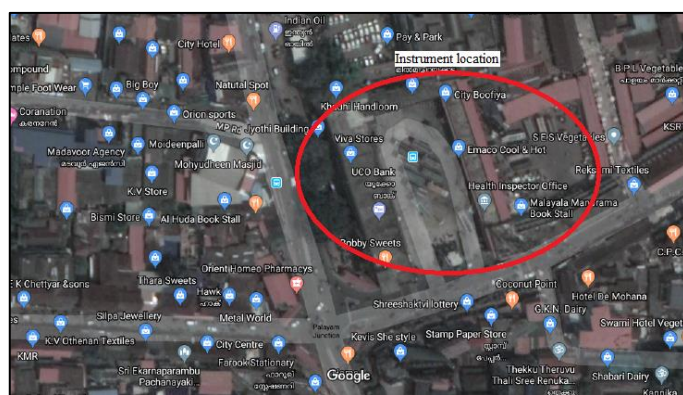
Non-invasive techniques for trace gas monitoring with high sensitivity and time resolution are available of which high finesse optical cavity methods like Cavity Enhanced Absorption Spectroscopy (CEAS) and Cavity Ring Down Spectroscopy (CRDs) are well established [Zheng et al., 2018; Nowakowaski et al., 2009]. These spectroscopic instruments are suitable for both laboratory and field measurements of the trace species as well as particulate matter with high accuracy [Wojtas et al., 2014; Ball et al., 2004; Ling et al., 2015]. Many trace gas measurement studies have been carried out around the world using incoherent broadband CEAS technique (IBBCEAS), since the time it has been first proposed [Fiedler et al., 2003]. A key advantage of IBBCEAS is multiple gas detection capability with high spatial and temporal resolution [Ruth et al., 2014], an important feature that makes the IBBCEAS popular and relevant methodology for *in-situ* trace gas monitoring. IBBCEAS has been used in wide spectral bands ranging from ultraviolet (UV) to near infrared (NIR) for various applications. To name a few: monitoring of molecular iodine [Dixneuf et al., 2008; Johansson et al., 2014], glyoxal [Washenfelder et al., 2008], IO and OIO [Vaughan et al., 2008], and NO_2 [Chandran et al., 2017; Langridge et al., 2006; Triki et al., 2008; Liang et al., 2017] using the visible spectral range; HONO [Nakashima et al., 2017; Wu et al., 2012; Gherman et al., 2008; Duan J. et al., 2015], BrO [Chen et al., 2011], and gaseous elemental Hg [Darby et al., 2012] using the UV spectral range; different VOCs [Orphal, and Ruth, 2008; Denzer et al., 2009], and natural gas components [Prakash et al., 2018] using the near IR spectral range have been reported. Open-path IBBCEAS (OP-IBBCEAS) measurements in simulation chambers were reported for NO_2 and NO_3 [Venables et al., 2006; Varma et al., 2009] and recent field measurements using the same configuration has reported a detection sensitivity of ~ 40 pptv for NO_3 even in the presence of aerosol loading [Suhail et al., 2018].

Ambient measurements of NO_3 have been widely conducted in USA, China and Europe. [Langridge et al., 2008; Kennedy et al., 2011; Wang et al., 2017, Wang et al., 2013]. However, few such studies have been reported from urban locations of India. In this study, we describe the use of OP-IBBCEAS for *in-situ* measurements of nocturnal NO_3 radical in a medium sized coastal city of Calicut (Kozhikode) in southern state of Kerala, India. The location of the measurements was chosen where heavy vehicles such as buses and trucks were operated heavily, and in idle conditions at times. The instrument was installed 8.5 meter above ground level on the east wing of the oldest of the three bus terminals [11.2495° N, 75.7842° E] of the Palayam part of the city that is also adjacent to the main vegetable sorting cum market facility, both of which are busy from approximately 3 AM till about 8 PM. Measurement campaign was chosen for a one-week period during 31st October – 10th November, 2018, and the presence of NO_3 at high mixing ratios were observed for five nights. The instrument stability was very good throughout the campaign with minimal optical realignment and optimizations. The experimental setup, calibration, measurements and results are discussed in the following sections.



2 Experimental

The OP-IBBCEAS instrument was deployed over the Palayam bus terminal on top of its eastern wing of the main terminal. The location is proximate to air pollution from various human and vehicular activities. Adjacent to the bus terminal is a vegetable sorting cum market where supplies are initiated to other parts of the district of Calicut. Hence, high traffic of trucks, idling during loading and unloading of vegetables, add to the pollution in addition to the buses moving in and out of the terminal. The Calicut city railway station is 0.5 km away from this site and is also very close to a key business street of the city. Another air quality monitoring station (observatory), also operated in this same location, was making hourly averaged measurements of NO_x , O_3 , PM_{10} , $\text{PM}_{2.5}$, RH and temperature. Since, NO_3 formation is triggered by the presence of NO_2 and O_3 , and OP-IBBCEAS measurement sensitivity depends on aerosol loading [Ruth et al., 2014], these concurrent measurements were valuable additions to this measurement campaign. Figure 1(a) shows the Google map image of the location and Fig. 1(b) that of the bus terminal.



15 **Figure 1(a): Google map image of Palayam bus terminal (Red circle). Figure 1(b): View of the main Palayam bus terminal from the instrument location (Pic courtesy: Google map)**

The OP-IBBCEAS instrument was placed on the rooftop of the east wing of the bus terminal on a single aluminium profile platform 4 m long and 1 m high. The schematic depiction of the experimental setup is shown in Fig. 2. The optical resonator was achieved by using a pair of high reflective (HR) dielectric mirrors with a radius of curvature of 3 m and diameter of 25.4 mm (Layertec GmbH). The company specified reflectivity of the mirror is > 0.999 in the 620 -720 nm spectral range. The HR mirror pair was mounted inside a custom made mirror mounts that have provision for purge gas inlet as well as insertion of a low-loss optic (used for the mirror reflectivity calibration). A Xe-arc lamp that works with an optical power of 150 W was used as the light source. L1 and L2 are lenses used to collimate the diverging beam from the arc lamp and to focus the beam at the centre of the cavity. Plane aluminium mirrors (M1 and M2) of 50 mm diameter were used to direct the beam into the optical resonator. A 650 nm long-pass (Andover 650FS80-50) and a 700 nm short-pass (Thorlabs) filter combination were used to spectrally filter the light from the arc lamp to match mirror reflectivity range. Along with this, a



colour glass filter (Newport FSQ-KG5) was used to eliminate the IR emissions from the lamp. A TE-cooled spectrometer with CCD array (Ocean Optics, model QE Pro) featuring high signal-to-noise ratio was used as the detector, with a focusing optic (L3) collecting the cavity signal. A He-Ne laser (JDS Uniphase, USA) was used for preliminary cavity alignment, with two aluminium mirrors (M3 and M4) guiding the laser beam through the cavity.

5

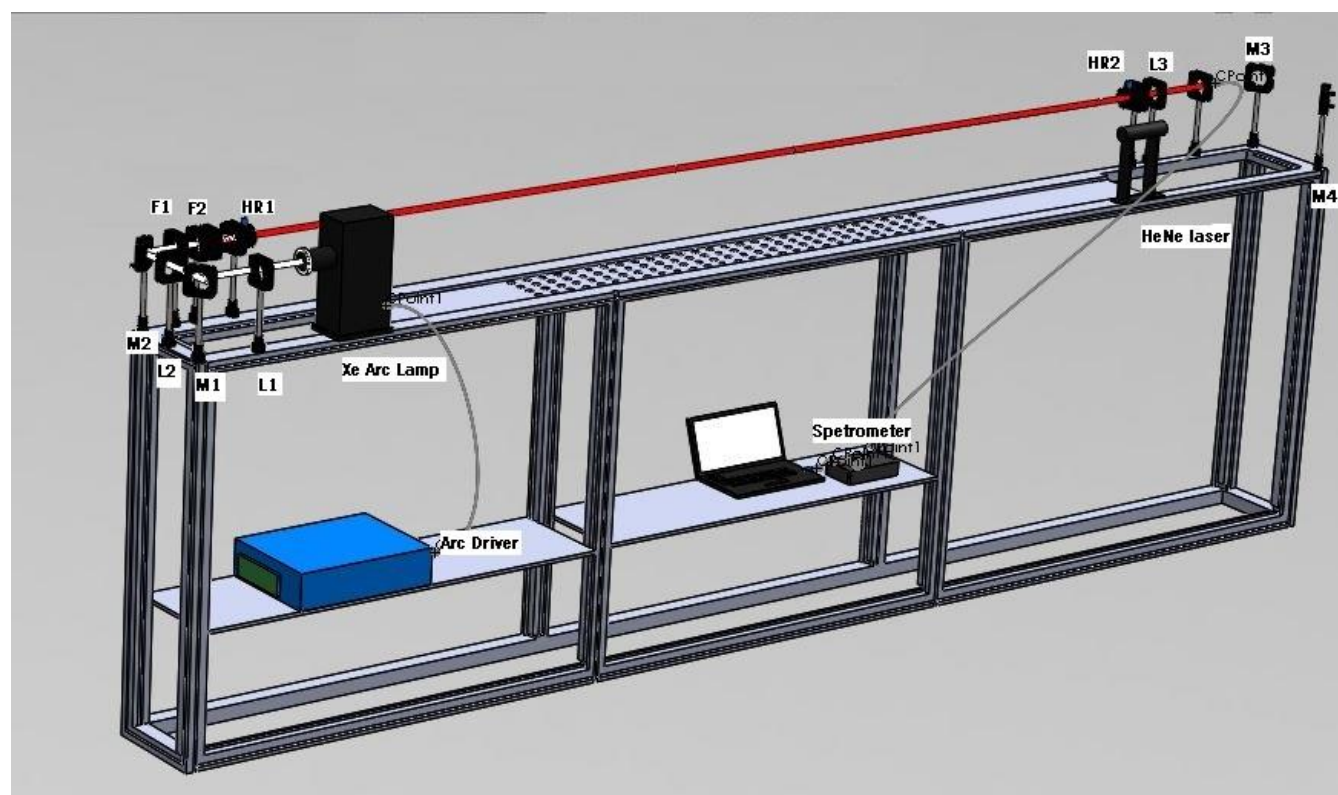


Figure 2: Schematic drawing of the OP-IBBCEAS setup on aluminium profile platform. HR1 and HR2 are high-reflectivity cavity mirrors. M1, M2, M3 and M4 are beam steering aluminium mirrors. L1, L2 are collimating lenses and L3 is the focusing lens to the fibre. F1 is the 650 long pass and 700 short pass filter combination and F2 is the the IR filter.

10

The length between two cavity mirrors was 285 cm. The cavity mirrors were purged by nitrogen gas at a rate of 100 mL/min for cavity mirror protection. The resolution of the spectrometer was determined to be 1.8 nm based on the FWHM of He-Ne laser line at 632.8 nm, and a Mercury-Argon calibration source (Ocean Optics, HG1) ascertained its wavelength calibration. A polyvinyl chloride (PVC) pipe 5 cm in diameter was connected between the cavity mirrors and N₂ was filled for acquisition of the reference spectrum (I_0) prior to measurements each night. A steady flow of nitrogen was maintained in atmospheric pressure during these measurements, which was achieved with the help of a manometer U-tube. The instrument calibration is the determination of the effective mirror reflectivity of the resonator. The calibration procedure was following previous studies [Varma et al., 2009; Suhail et al., 2018] by using a pre-calibrated low-loss optical window (Layertec

15



GmbH) with high transmission in the spectral range of the resonator. Soon after the reference spectrum was acquired, the low-loss optic was introduced into the optical path with nitrogen as background and effective mirror reflectivity was determined.

- 5 After the acquisition of I_0 and reflectivity calibration each night, the pipe was removed so that the cavity was open to ambient air. Each spectrum collected thereafter (I) was recorded at 1 min interval. The IBBCEAS equation, described in Eq. (1) below was used to calculate the extinction coefficient spectra [Fiedler et al., 2003].

$$\alpha(\lambda) = \frac{1}{d} \left(\frac{I_0(\lambda)}{I(\lambda)} - 1 \right) (1 - R(\lambda)) \quad (1)$$

10

where d is the length of the resonator, R is the effective mirror reflectivity, I_0 and I are the reference cavity transmission intensity and the sample cavity transmission intensity respectively as recorded by the spectrometer. The NO_3 concentration was retrieved from the cavity signal by fitting each spectrum with the sum of a quadratic polynomial baseline and the product of the number concentrations and absorption cross-sections of NO_3 [Yokelson et al., 1994], NO_2 [Vandaele et al., 1998] and water vapour [Rothman et al., 2005]. The fitting equation describes in Eq. (2) below was used [Varma et al., 2009],

15

$$\alpha(\lambda) = a_0 + a_1\lambda + a_2\lambda^2 + a_3\sigma_{\text{NO}_3}(\lambda) + a_4\sigma_{\text{NO}_2}(\lambda) + a_5\sigma_{\text{H}_2\text{O}}(\lambda) \quad (2)$$

20

where $\alpha(\lambda)$ is the extinction coefficient of the mixed sample, calculated from Eq. (1). σ_{NO_3} , σ_{NO_2} and $\sigma_{\text{H}_2\text{O}}$ (from HITRAN database) are the absorption cross-sections convolved to the resolution of the spectrometer. a_3 , a_4 and a_5 are the number densities of each species in the mixed sample and the first three terms of the equation accounts for the baseline offset of the extinction spectrum and the presence of O_3 in the sample.

25

Previous studies involving *in-situ* monitoring have reported issues with non-linear absorption of water vapour while retrieving NO_3 concentrations at lower resolutions when high-resolution HITRAN lines were convolved for least-square fitting [Bitter et al., 2005; Varma et al., 2009; Suhail et al., 2018]. In order to compensate for the non-linear Beer-Lambert behaviour, concentration-corrected absorption cross-section for water vapour was calculated from the average relative humidity (RH) and temperature (T) measurements obtained from the observatory. The water vapour concentration for the same was determined from RH and T following McRae (1980). A linear least square fit algorithm developed in MATLAB environment was used for the spectral fitting. The fit uncertainty returned by the algorithm was used as a measure of detection sensitivity in these measurements.

30



3 Results and Discussions

Urban Indian atmosphere is characterized by high rate of pollution with NO_x from vehicular exhaust, VOCs and O₃, in addition to particulate matter (PM). However, little effort had been visible in the literature studying the formation and destruction of NO₃, the most powerful nocturnal oxidant, in Indian urban environment. Invent of sensitive *in situ* detection techniques has made observation of the same graspable. Although a comprehensive and simultaneous monitoring of several reactive species is necessary to assess dynamics and transport of NO₃, observation of its presence at significant levels is highly relevant. In this study, the measurements were focussed during the night-time activities of heavy/medium diesel vehicles. During the week of observation about 120 such vehicles were active during 3 – 5 AM on each market day solely for sorting vegetables, and may have been the source of pollution for our observations. The activities close to the sorting facility (next to the instrument location) is roughly limited in a stretch of half km and the vehicles are left on idle during loading/unloading of vegetables. During normal working hours, this street south of the bus terminal, and the cross road to its west have high traffic of slow moving passenger vehicles (mostly cars and two-wheeler gasoline vehicles). The NO and NO₂ levels between 3 – 5 AM measured at the observatory located in the same terminal showed a minimum in daily values of ~20 and ~30 µg m⁻³ respectively (private communication). During daytime they peaked to ~120 and ~80 µg m⁻³ respectively on an average during the campaign period. These hourly observations were not analysed further for correlations due to the lack of comprehensive VOC measurements. During the measurement period significant wind was not prevailing, hence transport of pollutants from elsewhere was held negligible (~ 0.5 ms⁻¹ measured by anemometer at the observatory, mostly from the West that is from the direction of the coast).

The average effective mirror reflectivity (*R*) spectrum with standard deviation from all 5 days of measurement is shown in Fig. 3. The manufacturer specified reflectivity was > 0.999 in the spectral range of 620 – 720 nm. The actual reflectivity at 662 nm was determined to be ~0.9997.

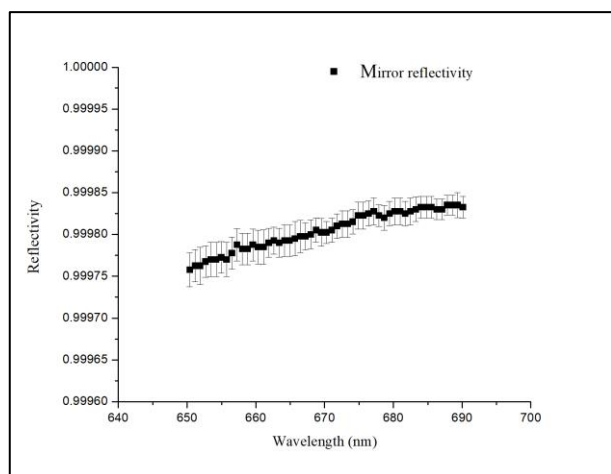




Figure 3: Mirror reflectivity (averaged over all 5 days of measurement). Error bar represents the standard deviation at corresponding wavelengths with a relative uncertainty of 3.2×10^{-5} at 662 nm.

Typical transmission spectra I_0 (red trace) and I (blue) trace are shown in Fig 4(a). The differences in the spectra are attributed to the presence of aerosol, water vapour and other atmospheric absorbing and scattering constituents. In fact, the acquisition of I spectrum in the figure was made at 10:15 PM on November 5th when the presence of NO_3 was detected. A mixing ratio of 40 pptv was retrieved with a fit uncertainty of 20 pptv.

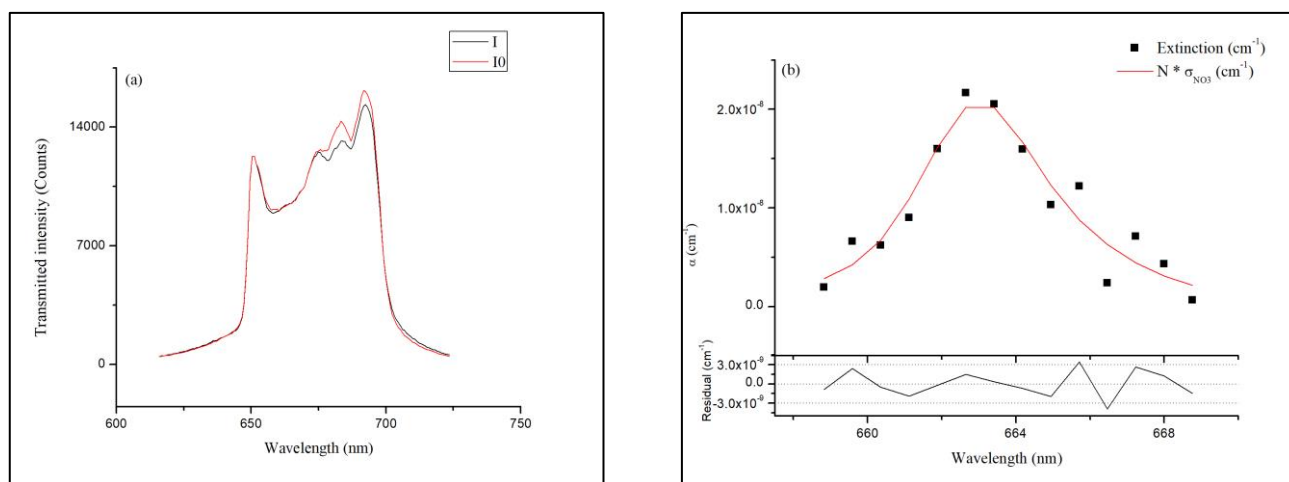


Figure 4: (a) Typical cavity transmission signal on day 4 when aerosol loading was relatively low. The red trace is the I_0 spectrum and the blue trace is the I spectrum when NO_3 was present at low levels (b) The absorption coefficient in 658 – 668 nm range showing NO_3 absorption alone (black square) with all other contributions (water vapour, NO_2 and a polynomial baseline) removed and its fit in red. Also shown is the fit residual. (The mixing ratio of NO_3 retrieved from this spectrum was 40 ± 20 pptv)

The RH values were fluctuating around 80% levels for most of the measurement period. The water cross-section spectrum in the spectral range of analysis was corrected for a corresponding concentration to account for nonlinear Beer-Lambert's behaviour throughout the campaign. During the whole week of campaign it was noticed that the vehicular activities start around 3 AM and remain busy till about 8 PM on every working day. Data acquisition after calibration was commenced from about 10 PM each night and continued till sunrise, which is about 6 AM in the morning at this location during the measurement period. A relatively calm period was observed during the night until after 2 AM. The NO_3 mixing ratio was observed to jump up shortly after the activities commence in the surroundings, and trucks running in idle engines may be a major source of pollution.

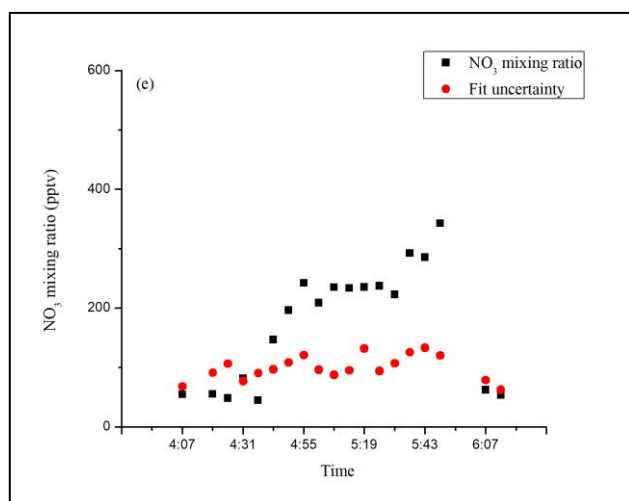
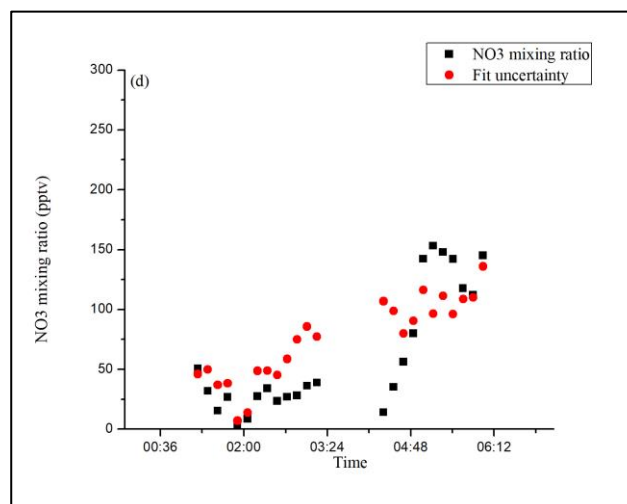
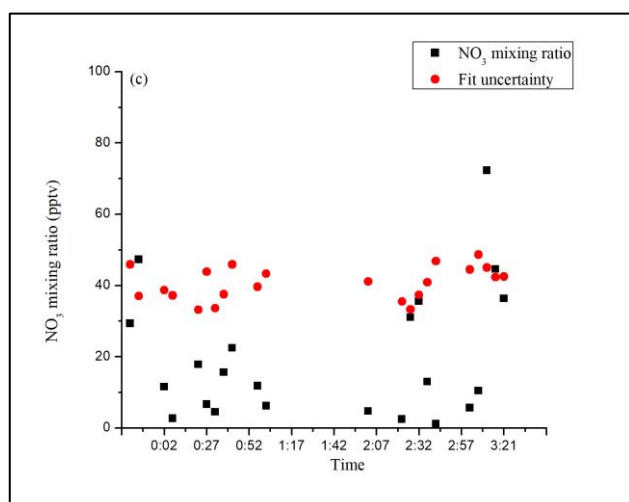
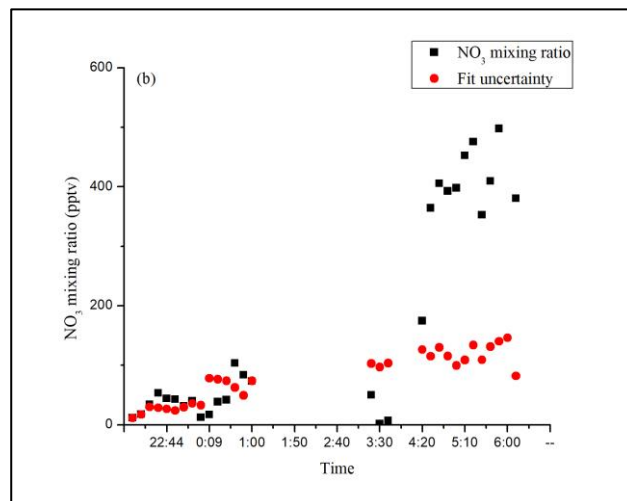
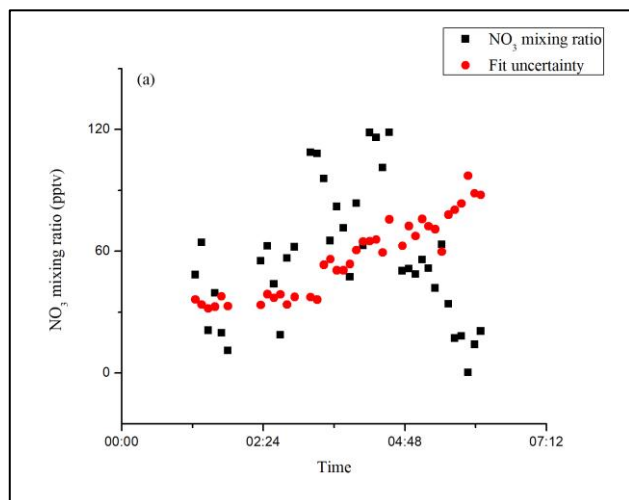




Figure 5: Time series of NO₃ mixing ratios in pptv from 5 nights of measurements (Black squares) with fit uncertainties (Red circles). It may be noticed that the fit uncertainty from analysis was in the range between a low value of ~20 pptv to a high value of ~100 pptv, the variation of which is attributed to variation in aerosol loading

5

Time series of the NO₃ mixing ratios (black) and uncertainty (red) retrieved from measurements for all five nights are shown in Fig 5. The presence of NO₃ is found to diminish immediately on day break every morning. Moderate levels of up to 120 pptv of NO₃ were measured on 31st October during the peak activity hours, as shown in fig. 5(a). The highest NO₃ concentration of 497 pptv was observed on the night of 5th November (immediately preceding sunrise on 6th morning) as can be seen from fig. 5(b). Figure 5(c) shows NO₃ concentration up to 60 pptv on the night of 6th November. On 8th November, the NO₃ peak concentration recorded was ~150 pptv and a steady raise after 3:00 A.M. was observed, as shown in fig. 5(d). Figure 5(e) illustrates the NO₃ concentration observed during the night of 10th November with a maximum of ~370 pptv.

Several *in-situ* measurements of NO₃ in short measurement campaigns have been made previously. We describe below a few of those measurements from different parts of the globe. Brown et al., 2007 made vertical distribution of NO₃ measurements in the nocturnal boundary layer in a semi-urban location near Boulder, USA, during 4 – 5 October, 2004. The measurements were made using Cavity Ring Down technique and mixing ratios of above 80 pptv were observed at ~200 m above the ground level.

20 Table 1. Observed NO₃ concentration in various locations with corresponding references

Location	Date	Measured maximum NO ₃ mixing ratio (pptv)	Method used	Reference
Boulder, USA	4 – 5 October 2004	< 100 pptv	CRDS	Brown et al. 2007
Beijing, China	February – May 2016	~ 50	IBBCEAS	Wang H et al., 2017
Hebei, China	28 -30 June 2014	~175	OP-IBBCEAS	Suhail et al., 2018
Thames Estuary, UK	July 2010	~200	IBBCEAS	Kennedy et al., 2011
Brittany, France	September 2006	< 100 (NO ₃ +N ₂ O ₅)	IBBCEAS	Langridge et al., 2008
Houston, USA	August – September 2000	~ 31 (at sunset)	DOAS	Gayer et al., 2003
Shanghai, China	August – October 2011	~95	DOAS	Wang S et al., 2013
Calicut, India	November 2018	~500	OP-IBBCEAS	This study

Differential Optical Absorption Spectroscopy (DOAS) was used by Gayer et al., 2003 for measuring daytime NO₃ in Houston, USA, as well as by Wang et al., 2013 for nocturnal measurements in Shanghai, China. IBBCEAS technique was used by Wang et al., 2017 in Beijing, China; by Kennedy et al., 2011 in Thames Estuary, UK; Langridge et al., 2008 in Brittany, France, and OP-IBBCEAS by Suhail et al., 2018 in Hebei, China. Many studies have reported a few hundreds of



pptv levels of nocturnal NO_3 , while our measurements in this study have seen a high of ~ 0.5 ppbv during one of the nights. In the absence of comprehensive VOC measurements source and sink apportionment is beyond the scope of this study, however, the measurements on 5th November showed the highest aerosol loading observed during this campaign coinciding with the highest NO_3 mixing ratio observed. Table 1 shows a comparison of previously reported measurements of ambient NO_3 in various locations with the present study.

It may be noted that the fit uncertainty levels are different for each night possibly due to the changes in aerosol loading. When the cavity was in open configuration (during measurements after calibration was completed each night) particulate matter (PM) suspended in the atmosphere filled the cavity thereby reducing the effective path lengths [Ruth et al., 2014] to some extent from the anticipated values. While aerosol loading was confirmed from the concurrent measurements of PM mass concentrations with corresponding reduction in our detection sensitivity (increase in uncertainty), we do not expect fluctuations on a time scale faster than our acquisition time as we are not immediately close to any fugitive PM emission sources.

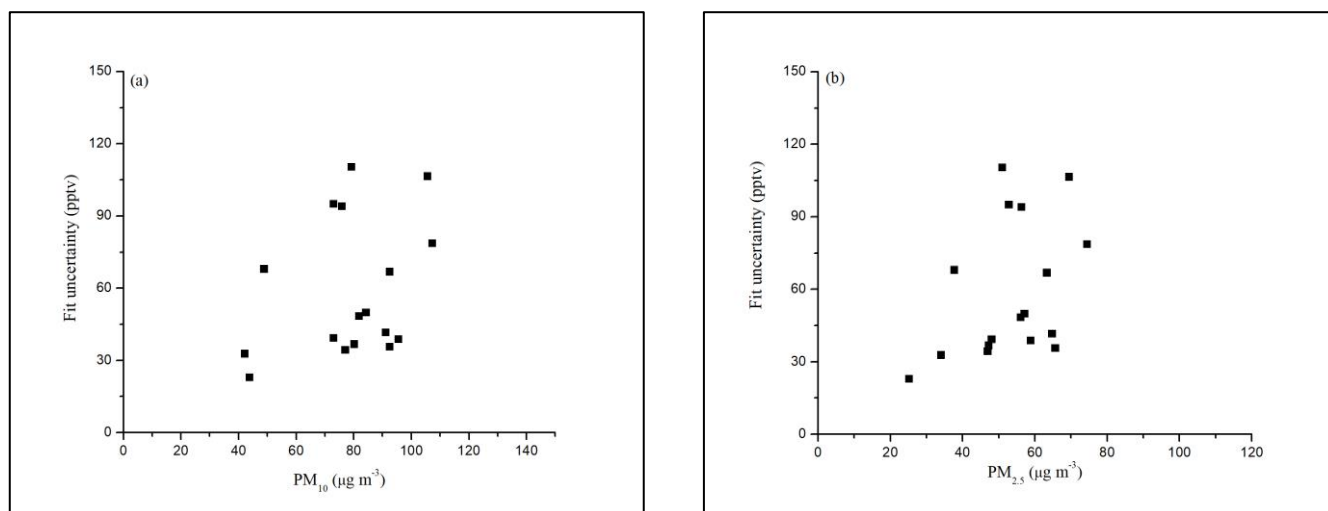


Figure 6: The scatterplots showing increase in uncertainty with increase in concentration of (a) PM_{10} and (b) $\text{PM}_{2.5}$.

It is to be noted that the measurement of R is made in aerosol free nitrogen atmosphere, giving an effective path length of $d \times (1-R)^{-1}$, where d is the cavity length. The measured reflectivity at 662 nm of ~ 0.9997 corresponds to an effective path length of ~ 9.5 km. In a previous study [Suhail et al., 2018], a slightly lower R of ~ 0.999 provided ~ 6.5 km effective path length in open-path configuration at a continental semi-urban location in China where moderate aerosol loading were present. The detection limit was ~ 40 pptv in that study and the variability in aerosol loading was minimal for the duration of measurements when compared to present study. As expected, increased R in the present study has not improved the detection



sensitivity appreciably because the attainable effective path length may have been limited by the atmospheric extinction due to high aerosol loading. In fact, the fit uncertainties were found to be higher during most nights, especially when noticeable increase in PM mass events occurred. The particulate mass concentrations (PM_{10} and $PM_{2.5}$) from concurrent measurements at the location from the nearby observatory (private communication) were used as indicators for aerosol loading and elevated fit uncertainty events from our instrument were checked against high aerosol loading events. An increase in concentration of either PM_{10} or $PM_{2.5}$ is indicative of an increase in atmospheric aerosol loading at the measurement location. The fit uncertainties were averaged for the same intervals of the hourly reported PM masses and plotted. An increase in the uncertainty with increase in PM_{10} and $PM_{2.5}$ may be inferred from the scatterplots in fig 6(a) and 6(b) respectively. The aerosol present in the atmosphere will be a mixture of species with optical properties ranging from non-absorbing to strongly absorbing. Therefore, a linear response to aerosol loading of fit uncertainty was not expected. Smaller particles may be dominated by sulphates and nitrates that are non-absorbing in this wavelength range and light extinction due to scattering may be dominant in such a scenario. Studies in similar environments have shown that roughly 40% of PM may be due to sum of elemental and organic carbon [Souza et al., 2014], in which case light extinction due to absorption may have added implication in the fit uncertainty. While a quantitative description of the dependence of the fit uncertainty on aerosol loading require size measurements, species-wise description of optical properties, and Mie calculations, it is noted that an increase in uncertainty results with general increase in aerosol loading.

4 Conclusions

This paper described the use of an OP-IBBCEAS system for *in-situ* detection of the most important nocturnal oxidant NO_3 in a middle-sized urban environment in India due to intense vehicular activities. The nocturnal atmospheric NO_3 radical was found to be present in moderate to high mixing ratios in the Indian city of Calicut (Kozhikode) when measured near a vegetable sorting facility and market where diesel vehicles were found idling. An IBBCEAS in open-path configuration (OP-IBBCEAS) was employed for monitoring NO_3 radical for a weeklong campaign of which data were available for 5 nights. The instrument was located on roof top of the east wing on Palayam bus terminal in the middle of Calicut city. The activities in the busy vegetable market started around 3.00 A.M. when truck movements were active. The results obtained from the measurements were consistent to these activities, with high NO_3 mixing ratios observed on all nights.

With an open optical cavity of 285 cm the effective mirror reflectivity of ~ 0.9997 at 662 nm was obtained in aerosol-free nitrogen atmosphere using a low-loss optical window of pre-calibrated loss. This corresponds to an effective pathlength of ~ 9.5 km. The stability of output intensity of the instrument was found to be excellent throughout the campaign with little need for optical realignments. High to moderate levels of NO_3 mixing ratios were found with a maximum of 497 pptv during the busy hours on 5th November when aerosol loading was high as well. On an average, the daily NO and NO_2 concentrations were found to be minimum at a level of ~ 20 and $\sim 30 \mu g m^{-3}$ respectively, when NO_3 measurements were at the highest levels. The minimum detection limit of the instrument was calculated from the fit uncertainty of the measured



NO₃ concentration and was found to vary in the 20 – 50 pptv range. The effect of aerosol loading on the fit uncertainty was studied from the hourly averaged concurrent PM_{2.5} and PM₁₀ mass measurements. The fit uncertainty was generally found to be increasing with increased aerosol loading, and has not reduced (to indicate improved sensitivity) with increased *R* when compared to a previous study [Suhail et al., 2014] in open-path configuration.

5

Author contribution: K. Suhail participated in planning and experimental activities, data analysis and manuscript preparation. R. Arun carried out the design of the instrument, participated in experiments, data analysis and manuscript preparation. J. Shreya prepared analysis program, carried out the data analysis and participated in manuscript preparation. J. Shebin, S. Aishwarya and P. Anoop participated in the experiment. R. Varma and V. Deepa were involved as investigators as well as participated in experiment planning and general supervision.

10

Acknowledgements: The authors thankfully acknowledge financial support from the Kerala State Council for Science, Technology and Environment, project code “003/SRSPS/2015/CSTE”. We are indebted to Prof. A. A. Ruth for loaning several components for the experiments. We are also grateful to Mr. Akhil V. M. and Mr. Shafeel K. U. for the assistance received in components fabrication.

15

References

- Atkinson, R.: Kinetics and mechanism of the gas-phase reactions of the NO₃ radical with organic compounds, *J. Phys. Chem. Ref. Data*, 20, 459–507, doi: 10.1063/1.555887, 1991.
- 20 Ball, S.M., Langridge, J.M., Jones, R.L.: Broadband cavity enhanced absorption spectroscopy using light emitting diodes, *Chem. Phys. Lett.*, 398, 68-74, 2004.
- Bitter, M., Ball, S.M., Povey, I.M., and Jones, R.L.: A broad-band cavity ringdown spectrometer for *in situ* measurements of atmospheric trace gases, *Atmos. Chem. Phys.*, 5, 2547-2560, 2005.
- Bohn, B., Rohrer, F., Brauers, T., and Wahner, A.: Actinometric measurements of NO₂ photolysis frequencies in the atmosphere simulation chamber SAPHIR, *Atmos. Chem. Phys.*, 5, 493-503, 2005.
- 25 Brown, S.S., Dube, W.P., Osthoff, H.D., Wolfe, D.E., Angevine, W.M. and Ravishankara, A.R.: High resolution vertical distributions of NO₃ and N₂O₅ through the nocturnal boundary layer, *Atmos. Chem. Phys.*, 7, 139-149, 2007.
- Chandran, S., Puthukkudy, A., and Varma, R.: Dual-wavelength dual-cavity spectrometer for NO₂ detection in the presence of aerosol interference, *Appl. Phys. B*, 213, 1-8, doi: 10.1007/s00340-017-6789-5, 2017.
- 30 Chen, J., and Venables, D. S.: A broadband optical cavity spectrometer for measuring weak near-ultraviolet absorption spectra of gases, *Atmos. Meas. Tech.*, 4, 425-436, doi: 10.5194/amt-4-425-2011, 2011.
- Darby, S.B., Smith, P.D., and Venables, D.S.: Cavity-enhanced absorption using an atomic line source: application to deep-UV measurements, *Analyst*, 137, 2318-2321, doi: 10.1039/c2an35149h, 2012.



- Denzer, W., Hamilton, M.L., Hancock, G., Islam, M., Langley, C.E., Peverall, R., and Ritchie, G.A.D.: Near-infrared broad band cavity enhanced absorption spectroscopy using a superluminescent light emitting diode, *Analyst*, 134, 2220-2223, doi: 10.1039/b916807a, 2009.
- Dixneuf, S., Ruth, A.A., Vaughan, S., Varma, R.M.: The time dependence of molecular iodine emission from *Laminaria digitata*. *Atmos. Chem. Phys.*, 9, 823–829, 2009.
- 5 Duan, J., Qin, M., Fang, W., Ling, L.Y., Hu, R.Z., Lu, X., Shen, L.L., Wang, D., Xie, P.H., Liu, J.G., and Liu, W.Q.: Incoherent broadband cavity enhanced absorption spectroscopy for measurements of atmospheric HONO, *Acta Phys. Sin.*, 64, 222–229, 2015.
- Fiedler, S.E., Hese, A., and Ruth, A.A.: Incoherent broad-band cavity-enhanced absorption spectroscopy, *Chemical Physics Letters*, 371, 284-294, doi: 10.1016/S00009-2614(03)00263-X, 2003.
- 10 Geyer, A., Alicke, B., Ackermann, R., Martinez, M., Harder, H., Brune, W., Piero di Carlo, Williams, E., Jobson, T., Hall, S., Shetter, R., and Stutz, j.: Direct observations of daytime NO₃: Implications for urban boundary layer chemistry, 108, 4368 – 4378, doi: 10.1029/2002JD002967, 2003.
- Gherman, T., Venables, D.S., Vaughan, S., Orphal J., and Ruth, A.A.: Incoherent broadband cavity enhanced absorption 15 spectroscopy in the near-ultraviolet: Application to HONO and NO₂, *Environ. Sci. Technol.*, 42(3), 890-895, doi: 10.1021/es0716913, 2008.
- Johansson, O., Mutelle, H., Parker, A.E., Batut, S., Demaux, P., Schoemaeker, C., Fittschen, C.: Quantitative IBBCEAS measurements of I₂ in the presence of aerosols. *Appl. Phys. B*, 114, 421–432, 2014.
- Kennedy, O.J., Ouyang, B., Langridge, J.M., Daniels, M.J.S., Bauguitte, S., Freshwater, R., McLeod, M.W., Ironmonger, C., 20 Sendall, J., Norris, O., Nightingale, R., Ball, S.M., and Jones, R.L.: An aircraft based three channel broadband cavity enhanced absorption spectrometer for simultaneous measurements of NO₃, N₂O₅ and NO₂, *Atmos. Meas. Tech.*, 4, 1759–1776, doi: 10.5194/amt-4-1759-2011, 2011.
- Khan, M.A.H., Cooke, M.C., Utembe, S.R., Archibald, A.T., Derwent, R.G., Xiao, P., Percival, C.J., Jenkin, M.E., Morris, W.C., and Shallcross, D.E.: Global modeling of the nitrate radical (NO₃) for present and pre-industrial scenarios, 25 *Atmospheric Research*, 164-165, 347-357, doi: 10.1016/j.atmosres.2015.06.006, 2015.
- Langridge, J.M., Ball, S.M., Jones, R.L.: A compact broadband cavity enhanced absorption spectrometer for detection of atmospheric NO₂ using light emitting diodes, *Analyst*, 131, 916–922, doi: 10.1039/b605636a, 2006.
- Langridge, J.M., Ball, S.M., Shillings, A.J.L., Jones, R.L.: A broadband absorption spectrometer using light emitting diodes for ultrasensitive, in-situ trace gas detection, *Rev. Sci. Instrum.*, 79, 123110, doi: 10.1063/1.3046282, 2008.
- 30 Larin, I. K., and Kuskov, M. L.: Daytime and nighttime lifetimes of minor atmospheric components in the troposphere, *Russian Journal of Physical Chemistry B*, 8, 254-260, 2014.
- Liang, S.X.; Qin, M.; Duan, J.; Fang, W.; Li, A.; Xu, J.; Lu, X.; Tang, K.; Xie, P.H.; Liu, J.G. et al.: Airborne cavity enhanced absorption spectroscopy for high time resolution measurements of atmospheric NO₂, *Acta Phys. Sin.*, , 66, 74–81, 2017.



- Ling, L.Y., Xie, P.H., Lin, P.P., Huang, Y.R., Qin, M., Duan, J., Hu, R.Z., Wu, F.C.: A concentration retrieval method for incoherent broadband cavity-enhanced absorption spectroscopy based on O₂-O₂ absorption, *Acta Phys. Sin.*, 64, 82–88, doi: 10.7498/aps.64.130705, 2015.
- McRae, G.J.: A simple procedure for calculating atmospheric water vapor concentration, *Journal of the Air Pollution Control Association*, 30:4, 394-394, doi: 10.1080/00022470.1980.10464362, 1980.
- 5 Monks, P.S.: Gas-phase radical chemistry in the troposphere, *Chem. Soc. Rev.*, 34, 376-395, doi: 10.1039/b307982c, 2005.
- Nakashima, Y., and Sadanaga, Y.: Validation of in-situ Measurements of Atmospheric Nitrous Acid Using Incoherent Broadband Cavity-enhanced Absorption Spectroscopy. *Anal. Sci.*, 33, 519–524, 2017.
- Nowakowski, M., Wojtas, J., Bielecki, Z., and Mikolajczyk, J.: Cavity enhanced absorption spectroscopy sensor, *Acta Physica Polonica A*, 116, 363 – 367, 2009.
- 10 Orphal, J., Ruth, A.A.: High-resolution Fourier-transform cavity-enhanced absorption spectroscopy in the near-infrared using an incoherent broad-band light source, *Optics Express*, 16 (23), 19232-19243, 2008.
- Prakash, N., Ramachandran, A., Varma, R., Chen, J., Mazzoleni, C., and Du, K.: Near-infrared incoherent broadband cavity enhanced absorption spectroscopy (NIR-IBBCEAS) for detection and quantification of natural gas components, *Analyst*, 143, 3284-3291, doi: 10.1039/c8an00819a, 2018.
- 15 Rothman, L., Jacquemart, D., Barbe, A., Chris Benner, D., Birk, M., Brown, L., Carleer, M., Chackerian, C., Chance, K., Coudert, L. et al.: The HITRAN 2004 molecular spectroscopic database, *J. Quant. Spectrosc. Radiat. Transf.*, 96, 139–204, 2005.
- Ruth, A.A., Dixneuf, S., Raghunandan, R.: *Broadband Cavity-Enhanced Absorption Spectroscopy with Incoherent Light, Cavity-Enhanced Spectroscopy and Sensing*, Gagliardi, G., Looock, H.P., Eds., Springer: Berlin/Heidelberg, Germany, Volume 179, doi: 10.1007/978-3-642-40003-2, 2014.
- 20 Sarnat, S.E.: Health effects of Organic aerosols: Results from the Southeastern center for air pollution and epidemiology, U.S. EPA STAR Progress Review Meeting, Research Triangle Park, North California, 15th March 2016, 2016.
- Souza, D.Z., Vasconcellos, P.C., Lee, H., Aurela, M., Saarnio, K., Teinilä, K. and Hillamo, R.: Composition of PM_{2.5} and PM₁₀ collected at urban sites in Brazil, *Aerosol and Air Quality Research*, 14, 168-176, 2014.
- 25 Suhail, K., George, M., Chandran S., Varma, R., Venables, D.S., Wang, M., and Chen, J.: Open path incoherent broadband cavity-enhanced measurements of NO₃ radical and aerosol extinction in the North China Plain, *Spectrochimica Acta Part A*, 1386-1425, doi: 10.1016/j.saa.2018.09.023, 2018.
- Triki, M., Cermak, P., Mejean, G., and Romanini, D.: Cavity- enhanced absorption spectroscopy with a red LED source for NO_x trace analysis, *Appl. Phys. B*, 91, 195-201, doi: 10.1007/s00340-008-2958-x, 2008.
- 30 Vandaele, A. C., C. Hermans, P. C., Simon, M., Carleer, R., Colin, S., Fally, M.F., Mérienne, A., Jenouvrier, and Coquart, B.: Measurements of the NO₂ absorption cross-section from 42,000 cm⁻¹ to 10,000 cm⁻¹ (238–1000 nm) at 220 K and 294 K, *J. Quant. Spectrosc. Radiat. Transfer*, 59, 171–184, 1998.



- Varma, R.M., Venables, D.S., Ruth, A.A., Heitmann, U., Schlosser, E., Dixneuf, S.: Long optical cavities for open-path monitoring of atmospheric trace gases and aerosol extinction, *Appl. Opt.*, 48, 159–171, doi: 10.1364/AO.48.00B159, 2009.
- Vaughan, S., Gherman, T., Ruth, A.A., and Orphal, J.: Incoherent broad-band cavity enhanced absorption spectroscopy of the marine boundary layer species I2, IO and OIO, *Phys. Chem. Chem. Phys.*, 10, 4471–4477, doi: 10.1039/b802618a, 2008.
- Venables, D.S., Gherman, T., Orphal, J., Wenger, J.C., and Ruth, A.A.: High sensitivity in situ monitoring of NO₃ in an atmospheric simulation chamber using incoherent broadband cavity enhanced absorption spectroscopy, *Environ. Sci. Technol.*, 40, 6758 – 6763, 2006.
- Wang, H., Chen, J., and Lu, K.: Development of a portable cavity-enhanced absorption spectrometer for the measurement of ambient NO₃ and N₂O₅: Experimental set-up, lab characterizations, and field applications in a polluted urban environment, *Atmos. Meas. Tech.*, 10, 1465–1479, doi: 10.5194/amt-10-1465-2017, 2017.
- Wang, S., Shi, C., Zhou, B., Zhao, H., Wang, Z., Yang, S., and Chen, L.: Observation of NO₃ radicals over Shanghai, China, *Atmospheric Environment*, 70, 401–409, doi: 10.1016/j.atmosenv.2013.01.022, 2013.
- Washenfelder, R.A., Langford, A.O., Fuchs, H., Brown, S.S.: Measurement of glyoxal using an incoherent broadband cavity enhanced absorption spectrometer, *Atmos. Chem. Phys.*, 8, 7779–7793, 2008.
- Wayne, R. P., Barnes, I., Biggs, P., Burrows, J. P., Canosa-Mas, C.E., Hjorth, J., Le Bras, G., Moortgat, G. K., Perner, D., Poulet, G., Restelli, G., and Sidebottom, H.: The nitrate radical: Physics, chemistry, and the atmosphere, *Atmos. Environ.*, 25A, 1–206, 1991.
- Wojtas, J., Tittel, F.K., Stacewicz, T., Bielecki, Z., Lewicki, R., Mikolajczyk, J., Nowakowski, M., Szabra, D., Stefanski, P., and Tarka, J.: Cavity enhanced absorption spectroscopy and photoacoustic spectroscopy for human breath analysis, *Int. J. Thermophys.*, doi: 10.1007/s10765-014-1586-4, 2014.
- Wu, T., Chen, W., Fertein, E., Cazier, F., Dewaele, D., Gao, X.: Development of an open-path incoherent broadband cavity-enhanced spectroscopy based instrument for simultaneous measurement of HONO and NO₂ in ambient air, *Appl. Phys. B*, 106, 501–509, 2012.
- Yokelson, R.J., Burkholder, J.B., Fox, R.W., Talukdar, R.K., Ravishankara, A.R.: Temperature dependence of the NO₃ absorption spectrum, *J. Phys. Chem.* 98, 13144–13150, 1994.
- Zheng, K., Zheng, C., Zhang, Y., Wang, Y., and Tittel, F.K.: Review of incoherent broadband cavity enhanced absorption spectroscopy (IBBCEAS) for gas sensing, *Sensors*, 18, 3646 – 3671, doi: 10.3390/s18113646, 2018.